

Nodeless superconducting gap induced by a competing odd-parity Fulde-Ferrell-Larkin-Ovchinnikov superconductivity in deeply underdoped cuprates

Tanmoy Das

Theoretical Division, Los Alamos National Laboratory, Los Alamos, NM 87545, USA

(Dated: September 1, 2022)

We develop a microscopic theory to show that the transition from an antiferromagnetic (AFM) phase to $d_{x^2-y^2}$ -wave superconductivity occurs through the robust companion of a triplet superconductivity. More interestingly, the symmetry combination of AFM and d -wave superconducting (SC) phase prescribes the triplet state to be odd parity and Fulde-Ferrell-Larkin-Ovchinnikov (FFLO) type with its center-of-mass momentum being single valued at the AFM wavevector $\mathbf{Q} = (\pi, \pi)$. Furthermore, the FFLO state produces a fully gapped quasi-particle spectrum which explains the recent observations of the ‘insulating’-like electronic structure of lightly doped cuprates in hole doping side. We have studied the stability of all three phases within the coupled self-consistent mean-field theory. Finally, we calculate the superfluid density to propose its exponential temperature dependence as a test to the SC origin of this ‘insulating’ state, while the phase modulation of the FFLO state can be visualized by scanning probes. The results are generic to all unconventional SC pairing symmetries including s^\pm in pnictide and others.

I. INTRODUCTION

A fascinating fact of cuprate research is that despite three decades of extensive research, experiments still uncover new and unexpected results which surprise our hitherto reached consensus. The latest addition to this investigation comes from various spectroscopic findings of a fully gapped or ‘insulating’-like electronic structure in deeply underdoped region,[1–7] where nodal d -wave pairing symmetry is expected. This feature is ubiquitously exhibited in many hole-doped cuprates studied so far, including La-based,[1, 5] Bi-based,[3, 4, 6] Cl-based,[2] and also Yb-based compounds.[7] This unexpected result led to essential questions such as: Is the fully gapped state related to superconductivity other than d -wave, or is it derived from the exotic normal state, or does it arise from the interplay of superconductivity with any normal state phase, or others?

Nodeless d -wave pairing state is demonstrated earlier to exist in electron-doped cuprates,[8] and also in 122 iron-chalcogenides.[9] However, in these cases either interaction or band structure topology removes the nodal states in the non-SC state itself, which thus yields a fully gapped electronic structure despite d -wave being the underlying pairing symmetry. But this description does not apply to the nodeless state in hole-doped systems since as temperature is raised above the SC state, a truncated Fermi surface (FS) is experimentally verified to exist in the nodal region.[5] Motivated by this unexpected behavior, several possible explanations have been put forward in recent times which include Coulomb disorder effect,[10] polaron effect,[6] $d + is$ pairing,[11] topological superconductivity,[12], dynamical mean-field theory calculations[13, 14]. However, no consensus is yet reached.

Our theory stems from the fact that the antiferromagnetic (AFM) phase of the parent compound persists up to the underdoped region and couples to superconductivity.[15–20] The evidence of the coexistence of AFM and SC in the underdoped region is well documented in numerous NMR,[15–18] neutron scattering[19, 20] data in multilayered Bi-based cuprates[15, 16] upto doping ~ 8 -12%, Tl- and Hg-based

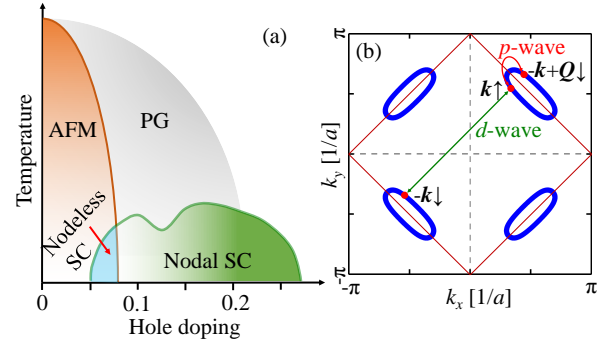


FIG. 1. (Color online) (a) Schematic (generalized) phase diagram of hole-doped cuprates. The light blue region is where fully gapped electronic state is documented, which in our view promotes a uniform coexistence of AFM and SC states with an unconventional FFLO phase. The doping value upto which AFM survives and coexists with SC is about 8-12% but somewhat materials dependent as measured by NMR, neutron scattering in various hole doped systems. [15–20] (b) Computed ‘normal’ state FS topology in the AFM state at $x \sim 0.08$. Solid brown line draws the magnetic BZ for the wavevector $\mathbf{Q} = (\pi, \pi)$ which is half of the paramagnetic BZ. Three representative Fermi momenta are highlighted which form zero and finite center of mass Cooper pairs.

cuprates[17] upto doping $\sim 10\%$, and Yb-based cuprates[18–20] upto doping ~ 8 -10%. Interestingly, the fully gapped state observed in these materials lies indeed within this doping range. Based on these data, we draw a generalized cuprate phase diagram as shown in Fig. 1(a). The interplay between the two competing interactions generically yields a dynamically generated new SC order parameter with finite center-of-mass. Earlier calculations predicted that for the competition of AFM and d -wave SC, the third SC order parameter is a nodal d -wave SC if no magnetic field is applied,[21, 22] or a time-reversal symmetry breaking π -triplet SC if a magnetic field is applied in the heavy-fermion systems[30]. Here we find that constrained by the symmetry consideration of the d -wave SC pairing symmetry and a single valued AFM ordering

vector $\mathbf{Q} = (\pi, \pi)$ in the cuprates, the third order parameter is an odd-parity superconductor which does not break time-reversal symmetry. Most interestingly, the dynamically generated triplet superconductivity is also nearest neighbor, as in the d -wave case, but it gives a fully gapped electronic structure which removes the nodes of the d -wave pairing. We develop a generic mean-field Hamiltonian based on the short range Coulomb repulsion and attractive potential to self-consistently evaluate all three coupled order parameters at a given doping. For experimental verification of our theory, we compute the temperature dependence of the superfluid density (inversely proportional to the square of the magnetic penetration depth) in the uniform coexistence state of all three interactions. We show that the exponential temperature dependence of the superfluid density will be a definitive test of the triplet SC origin of the apparent ‘insulating’ state in lightly doped cuprates. Furthermore, the amplitude modulation of the second SC gap can be directly visualized by scanning tunneling microscopy or spectroscopy (STM/STS).

II. THEORY

In the AFM state, the FS is reconstructed owing to the reduced Brillouin zone (BZ) defined by the modulation vector $\mathbf{Q} = (\pi, \pi)$ and the residual FS consists of small hole-pockets centering at the nodal points. The corresponding FS topology is shown in Fig. 1(b) for a realistic value of the AFM gap at doping $x \sim 0.08$ (see below). It is interesting to notice that when superconductivity appears in the new magnetic BZ, two types of Cooper pairs form. The typical d -wave Cooper pairs form between two electrons with opposite momenta and spin lying on different quadrant of the BZ as $\langle c_{\mathbf{k},\uparrow}^\dagger c_{-\mathbf{k},\downarrow}^\dagger \rangle$, where $c_{\mathbf{k},\uparrow}^\dagger$ is the fermionic creation operator at the crystal momentum \mathbf{k} with up spin (say). Additionally, two AFM quasiparticles $c_{\mathbf{k},\uparrow}^\dagger$ and $c_{-\mathbf{k}+\mathbf{Q},\downarrow}^\dagger$ lying inside and outside the magnetic BZ boundary, respectively, now become decoupled, and naturally form a second Cooper pairs with finite but single-valued center-of-mass momentum \mathbf{Q} as $\langle c_{\mathbf{k},\uparrow}^\dagger c_{-\mathbf{k}+\mathbf{Q},\downarrow}^\dagger \rangle$. Such Cooper pairs give Fulde-Ferrell-Larkin-Ovchinnikov (FFLO) type unconventional superconductivity originally proposed for Pauli limiting systems.[23] We lay out below a Ginzburg-Landau criterion to deduce the symmetry of the FFLO state in cuprates.

We now write down a mean-field based Hamiltonian for the single band case, relevant for most cuprates,[24–26] in which all aforementioned order parameters are treated on equal footing. The mean-field Hamiltonian is derived in the Appendix A from the full interacting Hamiltonian, and here we start with an effective Hamiltonian expressed in the Nambu-Gor’kov basis in the magnetic BZ $\Psi_{\mathbf{k}} = (c_{\mathbf{k},\uparrow}, c_{\mathbf{k}+\mathbf{Q},\uparrow}, c_{-\mathbf{k},\downarrow}^\dagger, c_{-\mathbf{k}+\mathbf{Q},\downarrow}^\dagger)$:

$$\langle \Psi_{\mathbf{k}}^\dagger | H | \Psi_{\mathbf{k}} \rangle = \begin{pmatrix} \xi_{\mathbf{k}} & -US & \Delta_{\mathbf{k}}^1 & \Delta_{\mathbf{k}}^2 \\ -US & \xi_{\mathbf{k}+\mathbf{Q}} & -\Delta_{\mathbf{k}}^{2*} & -\Delta_{\mathbf{k}}^1 \\ \Delta_{\mathbf{k}}^1 & -\Delta_{\mathbf{k}}^2 & -\xi_{\mathbf{k}} & -US \\ \Delta_{\mathbf{k}}^{2*} & -\Delta_{\mathbf{k}}^1 & -US & -\xi_{\mathbf{k}+\mathbf{Q}} \end{pmatrix}. \quad (1)$$

Here $\xi_{\mathbf{k}}$ is the non-interacting dispersion of the effective CuO_2 band expressed by tight-binding formalism in the Appendix A and the parameters are fitted to the $\text{La}_x\text{Sr}_{2-x}\text{CuO}_4$ (LSCO) dispersion.[27] U is the onsite Coulomb repulsion. The other three symbols S , and $\Delta_{\mathbf{k}}^{1/2}$ are the three mean-field order parameters for the AFM, d -wave and p -wave FFLO SC phase, respectively, as defined by $SN = \sum_{\mathbf{k},\sigma} \sigma \langle c_{\mathbf{k}+\mathbf{Q},\sigma}^\dagger c_{\mathbf{k},\sigma} \rangle$, $\Delta_{\mathbf{k}}^1 = \Delta_0^1 s_{\mathbf{k}} = V_0^1 s_{\mathbf{k}} \sum_{\mathbf{k}} s_{\mathbf{k}} \langle c_{\mathbf{k},\uparrow}^\dagger c_{-\mathbf{k},\downarrow}^\dagger \rangle$, and $\Delta_{\mathbf{k}}^2 = \Delta_0^2 p_{\mathbf{k}} = V_0^2 p_{\mathbf{k}} \sum_{\mathbf{k}} p_{\mathbf{k}} \langle c_{\mathbf{k}+\mathbf{Q},\uparrow}^\dagger c_{-\mathbf{k},\downarrow}^\dagger \rangle$. Here N is the number of lattice sites, and $V_0^{1/2}$ are the attractive interactions originate from the momentum dependence of the pairing interaction $V^1 = V_{\mathbf{k},-\mathbf{k}}$, and $V^2 = V_{\mathbf{k}+\mathbf{Q},-\mathbf{k}}$. $s_{\mathbf{k}} = \cos k_x - \cos k_y$ is the structure factor for $d_{x^2-y^2}$ -wave pairing symmetry, while that for the $p+ip$ -pairing is $p_{\mathbf{k}} = \sin k_x + i \sin k_y$. It is interesting to notice that both pairing symmetries transform in the same way under the particular choice of AFM wavevector \mathbf{Q} as $\Delta_{\mathbf{k}+\mathbf{Q}}^1 = -\Delta_{\mathbf{k}}^1$ and $\Delta_{\mathbf{k}+\mathbf{Q}}^2 = -\Delta_{\mathbf{k}}^{2*}$. The last identity also makes the triplet pairing respects time-reversal symmetry under this particular magnetic order. To see that we write down the Ginzburg-Landau type Free energy as:

$$F = \alpha [\Delta_0^1 (\Delta_0^{2*} \cdot \mathbf{S}) + \Delta_0^{1*} (\Delta_0^2 \cdot \mathbf{S})] + \dots, \quad (2)$$

where α is a constant and ‘...’ represents all the other quadratic, quartic and dipole coupling terms. It is interesting to notice that the staggered in-plane magnetic moment \mathbf{S} only allows the creation of a vector form of the FFLO pairing Δ_0^2 for a singlet SC order parameter Δ_0^1 . Furthermore, as mentioned before, since the time-reversed or the complex conjugate of Δ_0^2 lies outside the magnetic zone boundary with an opposite sign, the above coupling remains invariant under time-reversal symmetry. Finally, since superconductivity breaks gauge symmetry, while magnetism does not, the third order parameter must also break the gauge symmetry, i.e., the third order parameter must be a SC phase which allows the Hamiltonian to be gauge invariant. In this way, the commutator of any two order parameters generates the third one.

Returning back to our mean-field Hamiltonian in Eq. 1, we diagonalize it in three steps by using Bogolyubov transformation method. First we diagonalize the triplet SC gap with the change of basis as $c_{\mathbf{k}\uparrow} = f_{\mathbf{k}} t_{\mathbf{k},\uparrow} + g_{\mathbf{k}} t_{-\mathbf{k},\downarrow}^\dagger$, $c_{-\mathbf{k}\downarrow}^\dagger = g_{\mathbf{k}}^* t_{\mathbf{k},\uparrow} + f_{\mathbf{k}}^* t_{-\mathbf{k},\downarrow}^\dagger$, where $t_{\mathbf{k},\uparrow}$ is the Bogolyubov operator induced by Δ^2 -term, and the corresponding coherence factors are $2|f_{\mathbf{k}}|^2 = \left(1 + \frac{\xi_{\mathbf{k}}^+}{E_{\mathbf{k}}^\pi}\right)$, and $2|g_{\mathbf{k}}|^2 = \left(1 - \frac{\xi_{\mathbf{k}}^+}{E_{\mathbf{k}}^\pi}\right)$. The corresponding dispersion energies are $E_{\mathbf{k}}^\pi = \pm \sqrt{(\xi_{\mathbf{k}}^+)^2 + |\Delta_{\mathbf{k}}^2|^2}$, with $\xi_{\mathbf{k}}^\pm = (\xi_{\mathbf{k}} \pm \xi_{\mathbf{k}+\mathbf{Q}})/2$. In this new basis, the effective complex AFM gap and d -wave SC gap can be expressed by $\Delta_{\mathbf{k}}^m = (US\xi_{\mathbf{k}}^+ + \Delta_{\mathbf{k}}^2 \Delta_{\mathbf{k}}^1)/E_{\mathbf{k}}^\pi$, and $\Delta_{\mathbf{k}}^{\text{SC}} = (-\Delta_{\mathbf{k}}^1 \xi_{\mathbf{k}}^+ + \Delta_{\mathbf{k}}^2 US)/E_{\mathbf{k}}^\pi$. With the effective gaps, the above Hamiltonian reduces to a typical AFM+ d -SC phase which can now be diagonalized in the same fashion as done previously in Refs. 8 and 28, also see Appendix B. The corresponding effective AFM and SC coherence factors are $2|\alpha_{\mathbf{k}}|^2 = \left(1 + \frac{\xi_{\mathbf{k}}^-}{E_{\mathbf{k}}^m}\right)$, $2|\beta_{\mathbf{k}}|^2 = \left(1 - \frac{\xi_{\mathbf{k}}^-}{E_{\mathbf{k}}^m}\right)$, $2|u_{\mathbf{k}}^\pm|^2 = \left(1 + \frac{E_{\mathbf{k}}^\pi \pm E_{\mathbf{k}}^m}{E_{\mathbf{k}}^\pm}\right)$,

and $2|v_{\mathbf{k}}^{\pm}|^2 = \left(1 - \frac{E_{\mathbf{k}}^{\pi} \pm E_{\mathbf{k}}^m}{E_{\mathbf{k}}^{\pm}}\right)$. The quasiparticle energies are $(E_{\mathbf{k}}^{\pm})^2 = (E_{\mathbf{k}}^{\pi} \pm E_{\mathbf{k}}^m)^2 + |\Delta_{\mathbf{k}}^{\text{SC}}|^2$, where $E_{\mathbf{k}}^m = \sqrt{(\xi_{\mathbf{k}}^-)^2 + |\Delta_{\mathbf{k}}^m|^2}$. We evaluate all three order parameters and the chemical potential self-consistently for given values of constant interactions U , V_0^1 and V_0^2 at a given doping by solving the following coupled equations:

$$\begin{aligned}
SN &= \sum_{\mathbf{k}}' \alpha_{\mathbf{k}} \beta_{\mathbf{k}} (|f_{\mathbf{k}}|^2 - |g_{\mathbf{k}}|^2) \left[((v_{\mathbf{k}}^-)^2 - (v_{\mathbf{k}}^+)^2) \right. \\
&\quad \left. \times n(E_{\mathbf{k}}^+) - ((v_{\mathbf{k}}^-)^2 - (u_{\mathbf{k}}^-)^2) n(E_{\mathbf{k}}^-) \right], \quad (3) \\
\Delta_0^1 &= V_0^1 \sum_{\mathbf{k}}' \sum_{\nu=\pm} s_{\mathbf{k}} \left[\text{Re}[f_{\mathbf{k}}^2 - g_{\mathbf{k}}^2] u_{\mathbf{k}}^{\nu} v_{\mathbf{k}}^{\nu} \right. \\
&\quad \left. + 2\text{Re}[f_{\mathbf{k}} g_{\mathbf{k}}] \alpha_{\mathbf{k}} \beta_{\mathbf{k}} ((u_{\mathbf{k}}^{\nu})^2 - (v_{\mathbf{k}}^{\nu})^2) \right] \tanh(\beta E_{\mathbf{k}}^{\nu}/2) \lambda \neq \\
\Delta_0^2 &= V_0^2 \sum_{\mathbf{k}}' p_{\mathbf{k}} \sum_{\nu=\pm} \left[\text{Re}[f_{\mathbf{k}} g_{\mathbf{k}}] ((u_{\mathbf{k}}^{\nu})^2 - (v_{\mathbf{k}}^{\nu})^2) \right. \\
&\quad \left. + 2\alpha_{\mathbf{k}} \beta_{\mathbf{k}} u_{\mathbf{k}}^{\nu} v_{\mathbf{k}}^{\nu} (|f_{\mathbf{k}}|^2 - |g_{\mathbf{k}}|^2) \right] \tanh(\beta E_{\mathbf{k}}^{\nu}/2) \Big]. \quad (5)
\end{aligned}$$

Here the prime over a summation indicates that the summation is restricted within the magnetic BZ. $n(E_{\mathbf{k}}^{\nu})$ is the Fermi-Dirac

function.

For $U = 3t$ (t is the nearest neighbor tight-binding hopping parameter), $V_0^{1/2} = -87, -60$ meV, we get $S=0.1$, $\Delta_0^{1/2} = -20, -10$ meV, respectively at doping $x=0.08$ in LSCO which are realistic gap values for this material.[5] The resulting normal state FS is shown in Fig. 1(b). However, to facilitate the visualization of the nature of gap openings in the electronic structure, we use artificially large value of $\Delta_0^1=100$ meV and $\Delta_0^2=50$ meV in Fig. 2(a). In the presence of three competing interactions, the CuO_2 antibonding band splits into four quasiparticle states with finite gap at everywhere in the BZ. The bands are colored with corresponding filling factor which adds to 1 at each momentum. At the nodal point, the band gap is purely determined by the FFLO pairing, since a AFM+ d -wave pairing gives nodal states there. And the gap at the antinodal region is a mixture of all three gaps determined by $\sqrt{|\Delta_{\mathbf{k}}^m|^2 + |\Delta_{\mathbf{k}}^{\text{SC}}|^2}$.

To experimentally verify the SC origin of the fully gapped state, we calculate the penetration depth ($\lambda(T)$) or superfluid density via linear response theory by accounting for both the diamagnetic current (proportional to number of SC quasiparticles) and residual paramagnetic current (carried by normal state electrons) due to external magnetic field. The detailed derivation is given in the Appendix C, and we here write down the final expression:

$$\lambda_{ij}^{-2}(T) = \frac{4\pi e^2}{c^2 \Omega} \sum_{\mathbf{k}, \nu=\pm} \left[\left(\frac{1}{M_{\mathbf{k}i,j}^{\nu}} \right) \left(1 - \frac{E_{\mathbf{k}}^{\pi} + E_{\mathbf{k}}^m}{E_{\mathbf{k}}^{\nu}} \tanh(\beta E_{\mathbf{k}}^{\nu}/2) \right) + \left(\frac{1}{m_{\mathbf{k}i,j}^{\nu}} \right) \tanh(\beta E_{\mathbf{k}}^{\nu}/2) - \frac{\beta}{2} V_{\mathbf{k}i}^{\nu} V_{\mathbf{k}j}^{\nu} \text{sech}^2(\beta E_{\mathbf{k}}^{\nu}/2) \right]. \quad (6)$$

Here e , c are bare electronic charge and speed of light respectively, and Ω is the unit cell volume. M , m , and V are different band masses, and velocity defined in Appendix C. Due to C_4 symmetry in the system, the cross-terms are zero and the penetration depth matrix is diagonal. Therefore, we plot $\lambda_{xx}^{-2}(T)$ component only in Fig. 4 and normalized to its zero- T value.

III. RESULTS

A spectroscopic method to differentiate between the SC and magnetic origins of the nodal gap is to observe whether the gapped quasiparticle state has a band-folding or band-bending at the magnetic zone boundary or at the normal state Fermi momentum. To directly compare our result with the angle-resolved photoemission spectroscopy (ARPES) data, we compute the single-particle spectral weight along the nodal direction as shown in Fig. 2(b), while Fig. 2(c) is the ARPES data[5] for the same sample. In both cases, we see that the band folding (indicated by vertical arrows) occurs at a momentum which is far below the magnetic BZ boundary at $\mathbf{k} = (\pi/2, \pi/2)$ point (red line). The additional band appears

in the theory is a shadow band induced by the SC order, and possess much weak intensity when the SC gap is reduced to the realistic value of $\Delta_0^2 \sim 10$ meV.

In Fig. 3(a), we plot the extracted band gap (not the individual order parameters) as a function of FS angle (ϕ) measured with respect to the $k_x = \pi$ axis centering at $\mathbf{M} = (\pi, \pi)$ point. We see that in the non-superconducting AFM semimetallic state ($\Delta_0^{1,2} = 0$, but S =finite), gapless Fermi pocket exists in the region of $\phi \sim 22^\circ - 45^\circ$. The corresponding hole-pocket FS is also seen in the ARPES data for the same sample at much above the SC transition temperature T_c [reproduced from Ref. 5 in Fig. 3(b)]. In case of a pure d -wave SC without any triplet component ($\Delta_0^2 = 0$ and the other two order parameters are finite), the electronic state is gapped throughout the BZ expect at $\phi = 45^\circ$. The non-monotonic nature of the band gap is reproduced in such case and has been observed in ARPES measurements (see, e.g., Ref. 28). However, when the triplet component is turned on, a finite gap opens everywhere as described by $\sqrt{|\Delta_{\mathbf{k}}^m|^2 + |\Delta_{\mathbf{k}}^{\text{SC}}|^2}$. It is interesting to notice that the odd-parity triplet SC of present form is fully gapped throughout the BZ [see *inset* to Fig. 3(a)], regardless of the topology of the underlying FS and is argued to be topo-

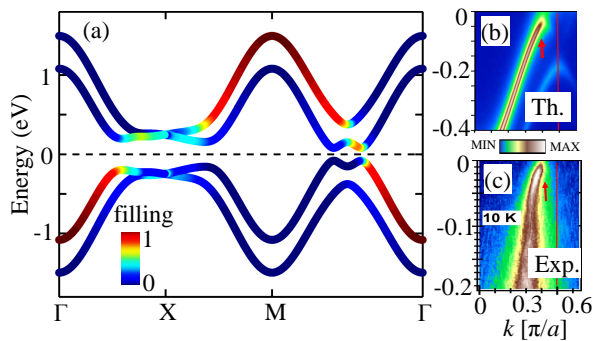


FIG. 2. (Color online) (a) Computed electronic dispersion in the coexistence state of AFM, d -wave SC and FFLO type $p + ip$ -wave SC. (b) Spectral weight map of the same spectrum along the nodal direction, exhibiting the location of band bending far below the magnetic BZ (arrows). The red vertical line marks the magnetic BZ boundary along the nodal axis. This result is consistent with the experimental observation of the same system, reproduced in (c) from Ref. 5.

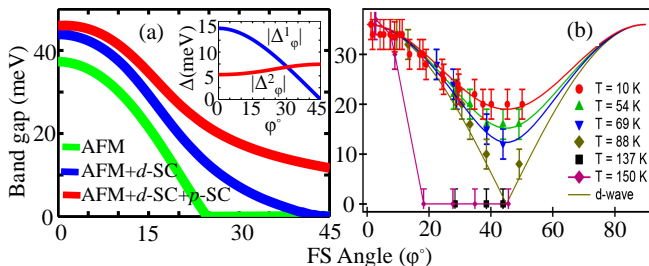


FIG. 3. (Color online) (a) Extracted band gap (not the order parameter) as a function of the FS angle ϕ° , where $\phi = 0^\circ$ and $\phi = 45^\circ$ give antinodal and nodal directions, respectively. (b) The corresponding experimental result, reproduced from Ref. 5 for the same sample, are in detailed agreement with the theory.

logically non-trivial if time-reversal symmetry is retained,[29] which is also applicable in the present case. The obtained gap structure agrees remarkably well with that observed in the ARPES measurement in the same sample as shown in Fig. 3(b) at low temperatures.

Finally, we compute the penetration depth for different cases of the competition of the phases under study to verify their existences in the underlying spectrum by using Eq. 6. It is well known that for a fully gapped superconductor, the inverse squared penetration depth $\lambda^{-2}(T)$ (proportional to the superfluid density) shows exponential T -dependence in the low- T region, where nodal d -wave SC exhibits a linear-in- T behavior, which sometimes modifies to the T^2 -dependence due to disorder.

To get a quantitative understanding, we calculate the temperature dependence of all gap values self-consistently at fixed values of the interaction parameters and at a fixed doping. Expectedly, we see that for a pure nodal d -wave ($\Delta^2 = 0$), the linear-in- T dependence of λ^{-2} is evident even in the presence of AFM ground state. With slowly turning on the fully gapped triplet pairing, the exponential dependence of λ^{-2} appears whose T -range of flat or exponential region depends on

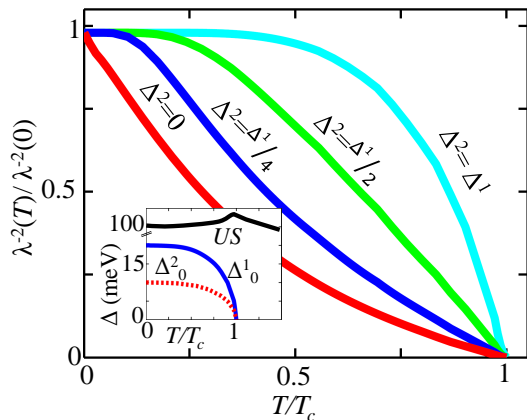


FIG. 4. (Color online) Computed $\lambda^{-2}(T)$ for several representative cases as indicated by adjacent labelling to each plot. Inset: Self-consistently calculated AFM gap, d - and p -wave gaps.

the relative strength of Δ^2/Δ^1 . For $\Delta^1 = \Delta^2$, the computed penetration depth shows a fully exponential behavior at all temperatures, which is a hallmark feature of s -wave like SC. The transition from a pure d -wave like $\lambda_{ij}^{-2}(T)$ behavior to nodeless d -wave behavior is reported in theory and experimental data of electron doped cuprates.[8] Since exponential behavior only appears in the very low-temperature (10-15

IV. CONCLUSION

In conclusion, the present paper provides a generalized framework for the phase stability of the AFM and d -wave superconductivity in hole-doped cuprates. We show that the uniform coexistence of these two phases is always accompanied by a third and robust triplet order parameter. The symmetry of the $\mathbf{Q} = (\pi, \pi)$ value AFM state and d -wave pairing restricts the symmetry of the triplet order parameter in cuprates to be odd-parity and FFLO type, which commences a fully gapped quasiparticle spectrum. The odd-parity order parameter breaks spin-rotational symmetry, but via coupling to the AFM state, it respects time-reversal symmetry. Interestingly, such a fully gapped odd parity pairing symmetry in a time-reversal invariant condition is called topological superconductor.[29] In general, such FFLO term can be expected to be negligibly small, however, the critical fluctuations of the parent phases can significantly enhance the strength of the triplet pairing interaction. While FFLO type SC has been proposed in many Pauli limited superconductors, such as nodal d -wave in CeCoIn₅ at high magnetic field,[30] and p -wave in the Rashba-type spin-orbit coupling systems without any realization to date, underdoped cuprates provide a clean and zero field platform to discover this exotic phase, if exists.

ACKNOWLEDGMENTS

The author acknowledges valuable discussions with X.-J. Zhou, C. Batista, and B. Altunkaynak. I also thank C.

Panagopolous for suggesting several references for the The work is supported by the U.S. DOE through the Office of Science (BES) and the LDRD Program and facilitated by NERSC computing allocation.

Appendix A: Derivation of the Hamiltonian

From the study of the group algebra[22, 31], it is obvious that the coexistence of the any two non-commutating order parameter produce a third order parameter. In case of AFM and d -superconductivity, there should be a third, dynamically generated, order parameter.[32] The strength of this third order parameter is subjects to the corresponding coupling constant. In the present work, we develop the theory for how the coexistence of AFM and d -wave superconductivity can generate a triplet and non-zero center of mass superconducting order parameter. Our starting Hamiltonian is

$$\begin{aligned}
H = & \sum_{\mathbf{k},\sigma} \xi_{\mathbf{k}} c_{\mathbf{k},\sigma}^{\dagger} c_{\mathbf{k},\sigma} + \frac{U}{N} \sum_{\mathbf{k},\mathbf{k}'} c_{\mathbf{k},\uparrow}^{\dagger} c_{\mathbf{k}+\mathbf{Q},\uparrow} c_{\mathbf{k}',\downarrow}^{\dagger} c_{\mathbf{k}-\mathbf{Q},\downarrow} \\
& + \sum_{\mathbf{k},\mathbf{k}'} V^1(\mathbf{k},\mathbf{k}') c_{\mathbf{k},\uparrow}^{\dagger} c_{-\mathbf{k},\downarrow}^{\dagger} c_{-\mathbf{k}',\downarrow} c_{\mathbf{k}',\uparrow} \\
& + \sum_{\mathbf{k},\mathbf{k}'} V^2(\mathbf{k},\mathbf{k}') c_{\mathbf{k},\uparrow}^{\dagger} c_{-\mathbf{k}-\mathbf{Q},\downarrow}^{\dagger} c_{-\mathbf{k}'-\mathbf{Q},\downarrow} c_{\mathbf{k}',\uparrow}.
\end{aligned} \tag{A1}$$

Here $\xi_{\mathbf{k}}$ is the bare dispersion, U is the onsite Coulomb interaction, $V^{1,2}$ are the pairing strengths for d -wave and p -

wave superconductivity, and N is the number of sites. We model the bare dispersion in the tight-binding form as $\xi_{\mathbf{k}} = -2t(\cos k_x + \cos k_y) - 4t' \cos k_x \cos k_y - 2t''(\cos 2k_x + \cos 2k_y) - 4t'''(\cos 2k_x \cos k_y + \cos k_x \cos 2k_y) - E_F$, where $(t, t', t'', t''', E_F) = (250, -25, 12, 35, -155)$ in eV which is obtained by fitting to the dispersion obtained by ARPES in LSCO.[27] $c_{\mathbf{k},\sigma}$ is the fermion annihilation operator at crystal momentum \mathbf{k} with spin $\sigma = \pm$. $\mathbf{Q} = (\pi, \pi)$ is the AFM nesting vector in 2D. We assume here a commensurate AFM so that $\mathbf{k} + \mathbf{Q} = \mathbf{k} - \mathbf{Q}$. The staggered spin magnetization is defined as $SN = \sum_{\mathbf{k},\sigma} \sigma \langle c_{\mathbf{k}+\mathbf{Q},\sigma}^{\dagger} c_{\mathbf{k},\sigma} \rangle$. For three order parameters, the crystal symmetry of them should be such that the commutator of any two of them should give the third one[31]. For this reason, if V^1 is assumed to be singlet d -wave symmetry, the AFM state greentrees that V^2 should be triplet (see main text). So we get, the singlet interaction $V^1(\mathbf{k},\mathbf{k}') = V_0^1 s_{\mathbf{k}} s_{\mathbf{k}'}$ and $V^2(\mathbf{k},\mathbf{k}') = V_0^2 p_{\mathbf{k}} p_{\mathbf{k}'}$, where $s_{\mathbf{k}} = \cos k_x - \cos k_y$ and $p_{\mathbf{k}} = \sin k_x + i \sin k_y$. We assume that $V^{1,2}$ are attractive. Then the SC order parameters are defined as, for singlet state, $\Delta_{\mathbf{k}'}^1 = \Delta_0^1 s_{\mathbf{k}'} = V_1 s_{\mathbf{k}'} \sum_{\mathbf{k}} s_{\mathbf{k}} \langle c_{\mathbf{k},\uparrow}^{\dagger} c_{-\mathbf{k},\downarrow}^{\dagger} \rangle = V_0^1 s_{\mathbf{k}'} \sum_{\mathbf{k}} s_{\mathbf{k}} \langle c_{\mathbf{k}+\mathbf{Q},\uparrow}^{\dagger} c_{-\mathbf{k}+\mathbf{Q},\downarrow}^{\dagger} \rangle$. On the other hand, the triplet order is decoupled in the main band and in the magnetic band as $\Delta_{\mathbf{k}'}^2 = \Delta_0^2 p_{\mathbf{k}'} = V_0^2 p_{\mathbf{k}'} \sum_{\mathbf{k}} p_{\mathbf{k}} \langle c_{\mathbf{k}+\mathbf{Q},\uparrow}^{\dagger} c_{-\mathbf{k},\downarrow}^{\dagger} \rangle$, while $\Delta_{\mathbf{k}'}^{2*} = V_0^2 p_{\mathbf{k}'} \sum_{\mathbf{k}} p_{\mathbf{k}} \langle c_{\mathbf{k},\uparrow}^{\dagger} c_{-\mathbf{k}+\mathbf{Q},\downarrow}^{\dagger} \rangle$. This is the reason why the time-reversal symmetry remains invariant in this triplet SC state. After substituting these mean-field orders, the total Hamiltonian reads,

$$\begin{aligned}
H = & \sum_{\mathbf{k},\sigma} \xi_{\mathbf{k}} c_{\mathbf{k},\sigma}^{\dagger} c_{\mathbf{k},\sigma} - US \sum_{\mathbf{k},\sigma} \sigma c_{\mathbf{k}+\mathbf{Q},\sigma}^{\dagger} c_{\mathbf{k},\sigma} + \sum_{\mathbf{k}} \Delta_{\mathbf{k}}^1 (c_{\mathbf{k},\uparrow}^{\dagger} c_{-\mathbf{k},\downarrow}^{\dagger} + c_{-\mathbf{k},\downarrow} c_{\mathbf{k},\uparrow}) + \sum_{\mathbf{k}} \Delta_{\mathbf{k}}^2 (c_{\mathbf{k},\uparrow}^{\dagger} c_{-\mathbf{k}-\mathbf{Q},\downarrow}^{\dagger} + c_{-\mathbf{k}-\mathbf{Q},\downarrow} c_{\mathbf{k},\uparrow}) \\
= & \sum_{\mathbf{k},\sigma} \xi_{\mathbf{k}}^+ (c_{\mathbf{k},\sigma}^{\dagger} c_{\mathbf{k},\sigma} + c_{\mathbf{k}+\mathbf{Q},\sigma}^{\dagger} c_{\mathbf{k}+\mathbf{Q},\sigma}) + \xi_{\mathbf{k}}^- (c_{\mathbf{k},\sigma}^{\dagger} c_{\mathbf{k},\sigma} - c_{\mathbf{k}+\mathbf{Q},\sigma}^{\dagger} c_{\mathbf{k}+\mathbf{Q},\sigma}) - 2US \sum_{\mathbf{k},\sigma} \sigma c_{\mathbf{k}+\mathbf{Q},\sigma}^{\dagger} c_{\mathbf{k},\sigma} \\
& + \sum_{\mathbf{k}} \Delta_{\mathbf{k}}^1 (c_{\mathbf{k},\uparrow}^{\dagger} c_{-\mathbf{k},\downarrow}^{\dagger} + c_{-\mathbf{k},\downarrow} c_{\mathbf{k},\uparrow} - c_{\mathbf{k}+\mathbf{Q},\uparrow}^{\dagger} c_{-\mathbf{k}-\mathbf{Q},\downarrow}^{\dagger} - c_{-\mathbf{k}-\mathbf{Q},\downarrow} c_{\mathbf{k}+\mathbf{Q},\uparrow}) \\
& + \sum_{\mathbf{k}} \Delta_{\mathbf{k}}^2 (c_{\mathbf{k},\uparrow}^{\dagger} c_{-\mathbf{k}-\mathbf{Q},\downarrow}^{\dagger} + c_{-\mathbf{k}-\mathbf{Q},\downarrow} c_{\mathbf{k},\uparrow} - c_{\mathbf{k}+\mathbf{Q},\uparrow}^{\dagger} c_{-\mathbf{k},\downarrow}^{\dagger} - c_{-\mathbf{k},\downarrow} c_{\mathbf{k}+\mathbf{Q},\uparrow}) + US^2 + \frac{|\Delta_0^1|^2}{V_0^1} + \frac{|\Delta_0^2|^2}{V_0^2}.
\end{aligned} \tag{A2}$$

The prime over the summation indicate that the sum is defined in the magnetic BZ. Defining a Nambu operator

$$\Psi_{\mathbf{k}} = \begin{pmatrix} c_{\mathbf{k},\uparrow} \\ c_{\mathbf{k}+\mathbf{Q},\uparrow} \\ c_{-\mathbf{k},\downarrow}^{\dagger} \\ c_{-\mathbf{k}-\mathbf{Q},\downarrow}^{\dagger} \end{pmatrix}$$

, one can define a 4×4 Hamiltonian matrix H as follows $\langle \Psi_{\mathbf{k}}^{\dagger} H \Psi_{\mathbf{k}} \rangle =$

$$\begin{pmatrix} (\xi_{\mathbf{k}}^+ + \xi_{\mathbf{k}}^-) & -US & \Delta_{\mathbf{k}}^1 & \Delta_{\mathbf{k}}^2 \\ -US & (\xi_{\mathbf{k}}^+ - \xi_{\mathbf{k}}^-) & -\Delta_{\mathbf{k}}^{2*} & -\Delta_{\mathbf{k}}^1 \\ \Delta_{\mathbf{k}}^1 & -\Delta_{\mathbf{k}}^2 & -(\xi_{\mathbf{k}}^+ + \xi_{\mathbf{k}}^-) & -US \\ \Delta_{\mathbf{k}}^{2*} & -\Delta_{\mathbf{k}}^1 & -US & -(\xi_{\mathbf{k}}^+ - \xi_{\mathbf{k}}^-) \end{pmatrix}$$

We diagonalize the above Hamiltonian in three steps by Bogolyubov transformation method. We first diagonalize the

triplet part, by the following unitary matrix,

$$\begin{pmatrix} c_{\mathbf{k},\uparrow} \\ c_{\mathbf{k}+\mathbf{Q},\uparrow} \\ c_{-\mathbf{k},\downarrow}^\dagger \\ c_{-\mathbf{k}-\mathbf{Q},\downarrow}^\dagger \end{pmatrix} = \begin{pmatrix} f_{\mathbf{k}} & 0 & 0 & -g_{\mathbf{k}} \\ 0 & f_{\mathbf{k}}^* & g_{\mathbf{k}}^* & 0 \\ 0 & -g_{\mathbf{k}} & f_{\mathbf{k}} & 0 \\ g_{\mathbf{k}}^* & 0 & 0 & f_{\mathbf{k}}^* \end{pmatrix} \begin{pmatrix} t_{\mathbf{k},\uparrow} \\ t_{\mathbf{k}+\mathbf{Q},\uparrow} \\ t_{-\mathbf{k},\downarrow}^\dagger \\ t_{-\mathbf{k}-\mathbf{Q},\downarrow}^\dagger \end{pmatrix}$$

where f and g are defined in the main text. SC gap become,

The Hamiltonian then transforms to $\langle \Psi_{\mathbf{k}}^\dagger H \Psi_{\mathbf{k}} \rangle =$

$$\begin{pmatrix} (E_{\mathbf{k}}^\pi + \xi_{\mathbf{k}}^-) & -\Delta_{\mathbf{k}}^m & \Delta_{\mathbf{k}}^{\text{SC}} & 0 \\ -\Delta_{\mathbf{k}}^m & (E_{\mathbf{k}}^\pi - \xi_{\mathbf{k}}^-) & 0 & -\Delta_{\mathbf{k}}^{\text{SC}} \\ \Delta_{\mathbf{k}}^{\text{SC}} & 0 & -(E_{\mathbf{k}}^\pi + \xi_{\mathbf{k}}^-) & -\Delta_{\mathbf{k}}^m \\ 0 & -\Delta_{\mathbf{k}}^{\text{SC}} & \Delta_{\mathbf{k}}^m & (E_{\mathbf{k}}^\pi - \xi_{\mathbf{k}}^-) \end{pmatrix}$$

$$\begin{pmatrix} t_{\mathbf{k},\uparrow} \\ t_{\mathbf{k}+\mathbf{Q},\uparrow} \\ t_{-\mathbf{k},\downarrow}^\dagger \\ t_{-\mathbf{k}-\mathbf{Q},\downarrow}^\dagger \end{pmatrix} = \begin{pmatrix} \alpha_{\mathbf{k}} u_{\mathbf{k}}^+ & \beta_{\mathbf{k}} u_{\mathbf{k}}^- & -\alpha_{\mathbf{k}} v_{\mathbf{k}}^+ & \beta_{\mathbf{k}} v_{\mathbf{k}}^- \\ -\beta_{\mathbf{k}} u_{\mathbf{k}}^+ & \alpha_{\mathbf{k}} u_{\mathbf{k}}^- & \beta_{\mathbf{k}} v_{\mathbf{k}}^+ & \alpha_{\mathbf{k}} v_{\mathbf{k}}^- \\ \alpha_{\mathbf{k}} v_{\mathbf{k}}^+ & \beta_{\mathbf{k}} v_{\mathbf{k}}^- & \alpha_{\mathbf{k}} u_{\mathbf{k}}^+ & -\beta_{\mathbf{k}} u_{\mathbf{k}}^- \\ \beta_{\mathbf{k}} v_{\mathbf{k}}^+ & -\alpha_{\mathbf{k}} v_{\mathbf{k}}^- & \beta_{\mathbf{k}} u_{\mathbf{k}}^+ & \alpha_{\mathbf{k}} u_{\mathbf{k}}^- \end{pmatrix} \begin{pmatrix} B_{\mathbf{k},\uparrow} \\ B_{\mathbf{k}+\mathbf{Q},\uparrow} \\ B_{-\mathbf{k},\downarrow}^\dagger \\ B_{-\mathbf{k}-\mathbf{Q},\downarrow}^\dagger \end{pmatrix}.$$

The AFM coherences factors α and β and the SC coherence factors u and v are also defined in the main text. Therefore,

All quantities here are defined in the main text. The above Hamiltonian looks same as in a AFM- d -SC state with effective AFM- and SC-gaps which is diagonalized by the following unitary matrix[28]

the total unitary matrix that diagonalizes the full Hamiltonian is

$$\hat{U}_{\mathbf{k}} = \begin{pmatrix} f_{\mathbf{k}} \alpha_{\mathbf{k}} u_{\mathbf{k}}^+ - g_{\mathbf{k}} \beta_{\mathbf{k}} v_{\mathbf{k}}^+ & f_{\mathbf{k}} \beta_{\mathbf{k}} u_{\mathbf{k}}^- + g_{\mathbf{k}} \alpha_{\mathbf{k}} v_{\mathbf{k}}^- & -f_{\mathbf{k}} \alpha_{\mathbf{k}} v_{\mathbf{k}}^+ - g_{\mathbf{k}} \beta_{\mathbf{k}} u_{\mathbf{k}}^+ & f_{\mathbf{k}} \beta_{\mathbf{k}} v_{\mathbf{k}}^- - g_{\mathbf{k}} \alpha_{\mathbf{k}} u_{\mathbf{k}}^- \\ -f_{\mathbf{k}}^* \beta_{\mathbf{k}} u_{\mathbf{k}}^+ + g_{\mathbf{k}}^* \alpha_{\mathbf{k}} v_{\mathbf{k}}^+ & f_{\mathbf{k}}^* \alpha_{\mathbf{k}} u_{\mathbf{k}}^- + g_{\mathbf{k}}^* \beta_{\mathbf{k}} v_{\mathbf{k}}^- & f_{\mathbf{k}}^* \beta_{\mathbf{k}} v_{\mathbf{k}}^+ + g_{\mathbf{k}}^* \alpha_{\mathbf{k}} u_{\mathbf{k}}^+ & f_{\mathbf{k}}^* \alpha_{\mathbf{k}} v_{\mathbf{k}}^- - g_{\mathbf{k}}^* \beta_{\mathbf{k}} u_{\mathbf{k}}^- \\ f_{\mathbf{k}} \alpha_{\mathbf{k}} v_{\mathbf{k}}^+ + g_{\mathbf{k}} \beta_{\mathbf{k}} u_{\mathbf{k}}^+ & f_{\mathbf{k}} \beta_{\mathbf{k}} v_{\mathbf{k}}^- - g_{\mathbf{k}} \alpha_{\mathbf{k}} u_{\mathbf{k}}^- & f_{\mathbf{k}} \alpha_{\mathbf{k}} u_{\mathbf{k}}^+ - g_{\mathbf{k}} \beta_{\mathbf{k}} v_{\mathbf{k}}^+ & -f_{\mathbf{k}} \beta_{\mathbf{k}} u_{\mathbf{k}}^- - g_{\mathbf{k}} \alpha_{\mathbf{k}} v_{\mathbf{k}}^- \\ f_{\mathbf{k}}^* \beta_{\mathbf{k}} v_{\mathbf{k}}^+ + g_{\mathbf{k}}^* \alpha_{\mathbf{k}} u_{\mathbf{k}}^+ & -f_{\mathbf{k}}^* \alpha_{\mathbf{k}} v_{\mathbf{k}}^- + g_{\mathbf{k}}^* \beta_{\mathbf{k}} u_{\mathbf{k}}^- & f_{\mathbf{k}}^* \beta_{\mathbf{k}} u_{\mathbf{k}}^+ - g_{\mathbf{k}}^* \alpha_{\mathbf{k}} v_{\mathbf{k}}^+ & f_{\mathbf{k}}^* \alpha_{\mathbf{k}} u_{\mathbf{k}}^- + g_{\mathbf{k}}^* \beta_{\mathbf{k}} v_{\mathbf{k}}^- \end{pmatrix}$$

Appendix B: Self-consistent order parameters

Now we derive the expression for the self-consistent order parameters in the eigenbasis.

$$\begin{aligned}
\Delta_0^1 &= V_0^1 \sum_{\mathbf{k}} s_{\mathbf{k}} \langle c_{\mathbf{k},\uparrow}^\dagger c_{-\mathbf{k},\downarrow}^\dagger \rangle = V_0^1 s_{\mathbf{k}'} \sum_{\mathbf{k}} s_{\mathbf{k}} \left[\langle c_{\mathbf{k},\uparrow}^\dagger c_{-\mathbf{k},\downarrow}^\dagger \rangle - \langle c_{\mathbf{k}+\mathbf{Q},\uparrow}^\dagger c_{-\mathbf{k}-\mathbf{Q},\downarrow}^\dagger \rangle \right] \\
&= V_0^1 \sum_{\mathbf{k}} s_{\mathbf{k}} \left[\left((f_{\mathbf{k}} \alpha_{\mathbf{k}} u_{\mathbf{k}}^+ - g_{\mathbf{k}} \beta_{\mathbf{k}} v_{\mathbf{k}}^+) (f_{\mathbf{k}} \alpha_{\mathbf{k}} v_{\mathbf{k}}^+ + g_{\mathbf{k}} \beta_{\mathbf{k}} u_{\mathbf{k}}^+) \langle B_{\mathbf{k},\uparrow}^\dagger B_{\mathbf{k},\uparrow} \rangle \right. \right. \\
&\quad + (f_{\mathbf{k}} \beta_{\mathbf{k}} u_{\mathbf{k}}^- + g_{\mathbf{k}} \alpha_{\mathbf{k}} v_{\mathbf{k}}^-) (f_{\mathbf{k}} \beta_{\mathbf{k}} v_{\mathbf{k}}^- - g_{\mathbf{k}} \alpha_{\mathbf{k}} u_{\mathbf{k}}^-) \langle B_{\mathbf{k}+\mathbf{Q},\uparrow}^\dagger B_{\mathbf{k}+\mathbf{Q},\uparrow} \rangle \\
&\quad + (-f_{\mathbf{k}} \alpha_{\mathbf{k}} v_{\mathbf{k}}^+ - g_{\mathbf{k}} \beta_{\mathbf{k}} u_{\mathbf{k}}^+) (f_{\mathbf{k}} \alpha_{\mathbf{k}} u_{\mathbf{k}}^+ - g_{\mathbf{k}} \beta_{\mathbf{k}} v_{\mathbf{k}}^+) \langle B_{-\mathbf{k},\uparrow}^\dagger B_{-\mathbf{k},\uparrow} \rangle \\
&\quad + (f_{\mathbf{k}} \beta_{\mathbf{k}} v_{\mathbf{k}}^- - g_{\mathbf{k}} \alpha_{\mathbf{k}} u_{\mathbf{k}}^-) (-f_{\mathbf{k}} \beta_{\mathbf{k}} u_{\mathbf{k}}^- - g_{\mathbf{k}} \alpha_{\mathbf{k}} v_{\mathbf{k}}^-) \langle B_{-\mathbf{k}+\mathbf{Q},\uparrow}^\dagger B_{-\mathbf{k}+\mathbf{Q},\uparrow} \rangle \left. \right) \\
&\quad - (-f_{\mathbf{k}}^* \beta_{\mathbf{k}} u_{\mathbf{k}}^+ + g_{\mathbf{k}}^* \alpha_{\mathbf{k}} v_{\mathbf{k}}^+) (f_{\mathbf{k}}^* \beta_{\mathbf{k}} v_{\mathbf{k}}^+ + g_{\mathbf{k}}^* \alpha_{\mathbf{k}} u_{\mathbf{k}}^+) \langle B_{\mathbf{k},\uparrow}^\dagger B_{\mathbf{k},\uparrow} \rangle \\
&\quad - (f_{\mathbf{k}}^* \alpha_{\mathbf{k}} u_{\mathbf{k}}^- + g_{\mathbf{k}}^* \beta_{\mathbf{k}} v_{\mathbf{k}}^-) (-f_{\mathbf{k}}^* \alpha_{\mathbf{k}} v_{\mathbf{k}}^- + g_{\mathbf{k}}^* \beta_{\mathbf{k}} u_{\mathbf{k}}^-) \langle B_{\mathbf{k}+\mathbf{Q},\uparrow}^\dagger B_{\mathbf{k}+\mathbf{Q},\uparrow} \rangle \\
&\quad - (f_{\mathbf{k}}^* \beta_{\mathbf{k}} v_{\mathbf{k}}^+ + g_{\mathbf{k}}^* \alpha_{\mathbf{k}} u_{\mathbf{k}}^+) (f_{\mathbf{k}}^* \beta_{\mathbf{k}} u_{\mathbf{k}}^+ - g_{\mathbf{k}}^* \alpha_{\mathbf{k}} v_{\mathbf{k}}^+) \langle B_{-\mathbf{k},\uparrow}^\dagger B_{-\mathbf{k},\uparrow} \rangle \\
&\quad \left. - (f_{\mathbf{k}}^* \alpha_{\mathbf{k}} v_{\mathbf{k}}^- - g_{\mathbf{k}}^* \beta_{\mathbf{k}} u_{\mathbf{k}}^-) (f_{\mathbf{k}}^* \alpha_{\mathbf{k}} u_{\mathbf{k}}^- + g_{\mathbf{k}}^* \beta_{\mathbf{k}} v_{\mathbf{k}}^-) \langle B_{-\mathbf{k}+\mathbf{Q},\uparrow}^\dagger B_{-\mathbf{k}+\mathbf{Q},\uparrow} \rangle \right] \\
&= V_0^1 \sum_{\mathbf{k}} \sum_{\nu=\pm} s_{\mathbf{k}} \left[\text{Re}[f_{\mathbf{k}}^2 - g_{\mathbf{k}}^2] u_{\mathbf{k}}^\nu v_{\mathbf{k}}^\nu + 2 \text{Re}[f_{\mathbf{k}} g_{\mathbf{k}}] \alpha_{\mathbf{k}} \beta_{\mathbf{k}} ((u_{\mathbf{k}}^\nu)^2 - (v_{\mathbf{k}}^\nu)^2) \right] \tanh(\beta E_{\mathbf{k}}^\nu / 2) \tag{B1}
\end{aligned}$$

In the first line and right hand side of the above equation we have taken into account of the fact that the d -wave structure factor $s_{\mathbf{k}+\mathbf{Q}} = -s_{\mathbf{k}}$ for this particular commensurate wavevector. Since we have identified $E_{\mathbf{k}}^\pm$ as the excitation energies of the fermion quasi-particles, the probability of its excitation in thermal equilibrium is the usual Fermi function,

$$\langle B_{\mathbf{k},\sigma}^\dagger B_{\mathbf{k},\sigma} \rangle = n(E_{\mathbf{k}}^+) = (\exp(\beta E_{\mathbf{k}}^+) + 1)^{-1}, \tag{B2}$$

with $\beta = 1/k_B T$ and so on. Therefore

$$\begin{aligned}
\langle 1 - B_{\mathbf{k},\sigma}^\dagger B_{\mathbf{k},\sigma} - B_{-\mathbf{k},\bar{\sigma}}^\dagger B_{-\mathbf{k},\bar{\sigma}} \rangle &= 1 - 2n(E_{\mathbf{k}}^+) \\
&= \tanh(\beta E_{\mathbf{k}}^+ / 2). \tag{B3}
\end{aligned}$$

The triplet SC order is

$$\begin{aligned}
\Delta_0^2 &= V_0^2 \sum_{\mathbf{k}} p_{\mathbf{k}} \langle c_{\mathbf{k},\uparrow}^\dagger c_{-\mathbf{k}-\mathbf{Q},\downarrow}^\dagger \rangle \\
&= V_0^2 \sum_{\mathbf{k}} \left[p_{\mathbf{k}} \langle c_{\mathbf{k},\uparrow}^\dagger c_{-\mathbf{k}-\mathbf{Q},\downarrow}^\dagger \rangle - p_{\mathbf{k}}^* \langle c_{\mathbf{k}+\mathbf{Q},\uparrow}^\dagger c_{-\mathbf{k},\downarrow}^\dagger \rangle \right]. \tag{B4}
\end{aligned}$$

As mentioned before, the difference between the triplet and singlet pairings in the magnetic Brillouin zone is that in the former case, the pairing symmetry picks up the complex conjugate as we go from the main band to the AFM subbands shifted by \mathbf{Q} vector, and also changes sign. Writing in Bogolyubov quasiparticle form as before, we get

$$\begin{aligned}
\Delta_0^2 &= V_0^2 \sum_{\mathbf{k}} \left[p_{\mathbf{k}} \left((f_{\mathbf{k}} \alpha_{\mathbf{k}} u_{\mathbf{k}}^+ - g_{\mathbf{k}} \beta_{\mathbf{k}} v_{\mathbf{k}}^+) (f_{\mathbf{k}}^* \beta_{\mathbf{k}} v_{\mathbf{k}}^+ + g_{\mathbf{k}}^* \alpha_{\mathbf{k}} u_{\mathbf{k}}^+) \langle B_{\mathbf{k},\uparrow}^\dagger B_{\mathbf{k},\uparrow} \rangle \right. \right. \\
&\quad + (f_{\mathbf{k}} \beta_{\mathbf{k}} u_{\mathbf{k}}^- + g_{\mathbf{k}} \alpha_{\mathbf{k}} v_{\mathbf{k}}^-) (-f_{\mathbf{k}}^* \alpha_{\mathbf{k}} v_{\mathbf{k}}^- + g_{\mathbf{k}}^* \beta_{\mathbf{k}} u_{\mathbf{k}}^-) \langle B_{\mathbf{k}+\mathbf{Q},\uparrow}^\dagger B_{\mathbf{k}+\mathbf{Q},\uparrow} \rangle \\
&\quad + (-f_{\mathbf{k}} \alpha_{\mathbf{k}} v_{\mathbf{k}}^+ - g_{\mathbf{k}} \beta_{\mathbf{k}} u_{\mathbf{k}}^+) (f_{\mathbf{k}}^* \beta_{\mathbf{k}} u_{\mathbf{k}}^+ - g_{\mathbf{k}}^* \alpha_{\mathbf{k}} v_{\mathbf{k}}^+) \langle B_{-\mathbf{k},\uparrow}^\dagger B_{-\mathbf{k},\uparrow} \rangle \\
&\quad + (f_{\mathbf{k}} \beta_{\mathbf{k}} v_{\mathbf{k}}^- - g_{\mathbf{k}} \alpha_{\mathbf{k}} u_{\mathbf{k}}^-) (f_{\mathbf{k}}^* \alpha_{\mathbf{k}} u_{\mathbf{k}}^- + g_{\mathbf{k}}^* \beta_{\mathbf{k}} v_{\mathbf{k}}^-) \langle B_{-\mathbf{k}+\mathbf{Q},\uparrow}^\dagger B_{-\mathbf{k}+\mathbf{Q},\uparrow} \rangle \left. \right) \\
&\quad - p_{\mathbf{k}}^* \left((-f_{\mathbf{k}}^* \beta_{\mathbf{k}} u_{\mathbf{k}}^+ + g_{\mathbf{k}}^* \alpha_{\mathbf{k}} v_{\mathbf{k}}^+) (f_{\mathbf{k}} \alpha_{\mathbf{k}} v_{\mathbf{k}}^+ + g_{\mathbf{k}} \beta_{\mathbf{k}} u_{\mathbf{k}}^+) \langle B_{\mathbf{k},\uparrow}^\dagger B_{\mathbf{k},\uparrow} \rangle \right. \\
&\quad + (f_{\mathbf{k}}^* \alpha_{\mathbf{k}} u_{\mathbf{k}}^- + g_{\mathbf{k}}^* \beta_{\mathbf{k}} v_{\mathbf{k}}^-) (f_{\mathbf{k}} \beta_{\mathbf{k}} v_{\mathbf{k}}^- - g_{\mathbf{k}} \alpha_{\mathbf{k}} u_{\mathbf{k}}^-) \langle B_{\mathbf{k}+\mathbf{Q},\uparrow}^\dagger B_{\mathbf{k}+\mathbf{Q},\uparrow} \rangle \\
&\quad + (f_{\mathbf{k}}^* \beta_{\mathbf{k}} v_{\mathbf{k}}^+ + g_{\mathbf{k}}^* \alpha_{\mathbf{k}} u_{\mathbf{k}}^+) (f_{\mathbf{k}} \alpha_{\mathbf{k}} u_{\mathbf{k}}^+ - g_{\mathbf{k}} \beta_{\mathbf{k}} v_{\mathbf{k}}^+) \langle B_{-\mathbf{k},\uparrow}^\dagger B_{-\mathbf{k},\uparrow} \rangle \\
&\quad \left. + (f_{\mathbf{k}}^* \alpha_{\mathbf{k}} v_{\mathbf{k}}^- - g_{\mathbf{k}}^* \beta_{\mathbf{k}} u_{\mathbf{k}}^-) (-f_{\mathbf{k}} \beta_{\mathbf{k}} u_{\mathbf{k}}^- - g_{\mathbf{k}} \alpha_{\mathbf{k}} v_{\mathbf{k}}^-) \langle B_{-\mathbf{k}+\mathbf{Q},\uparrow}^\dagger B_{-\mathbf{k}+\mathbf{Q},\uparrow} \rangle \right) \left. \right] \\
&= V_0^2 \sum_{\mathbf{k}} p_{\mathbf{k}} \sum_{\nu} \left[[\text{Re}[f_{\mathbf{k}} g_{\mathbf{k}}] ((u_{\mathbf{k}}^\nu)^2 - (v_{\mathbf{k}}^\nu)^2) + 2 \alpha_{\mathbf{k}} \beta_{\mathbf{k}} u_{\mathbf{k}}^\nu v_{\mathbf{k}}^\nu (|f_{\mathbf{k}}|^2 - |g_{\mathbf{k}}|^2)] \tanh(\beta E_{\mathbf{k}}^\nu / 2) \right]. \tag{B5}
\end{aligned}$$

Finally, the staggered magnetic is

$$\begin{aligned}
SN &= \sum_{\mathbf{k}, \sigma} \sigma \langle c_{\mathbf{k}+\mathbf{Q}, \sigma}^\dagger c_{\mathbf{k}, \sigma} \rangle = \sum_{\mathbf{k}} \left[\langle c_{\mathbf{k}+\mathbf{Q}, \uparrow}^\dagger c_{\mathbf{k}, \uparrow} \rangle - \langle c_{-\mathbf{k}-\mathbf{Q}, \downarrow}^\dagger c_{-\mathbf{k}, \downarrow} \rangle \right] \\
&= \sum_{\mathbf{k}} \left[\langle c_{\mathbf{k}+\mathbf{Q}, \uparrow}^\dagger c_{\mathbf{k}, \uparrow} \rangle + \langle c_{\mathbf{k}, \uparrow}^\dagger c_{\mathbf{k}+\mathbf{Q}, \uparrow} \rangle - \langle c_{-\mathbf{k}-\mathbf{Q}, \downarrow}^\dagger c_{-\mathbf{k}, \downarrow} \rangle - \langle c_{-\mathbf{k}, \downarrow}^\dagger c_{-\mathbf{k}-\mathbf{Q}, \downarrow} \rangle \right] \\
&= \sum_{\mathbf{k}} \left[(f_{\mathbf{k}} \alpha_{\mathbf{k}} u_{\mathbf{k}}^+ - g_{\mathbf{k}} \beta_{\mathbf{k}} v_{\mathbf{k}}^+) (-f_{\mathbf{k}}^* \beta_{\mathbf{k}} u_{\mathbf{k}}^+ + g_{\mathbf{k}}^* \alpha_{\mathbf{k}} v_{\mathbf{k}}^+) \langle B_{\mathbf{k}, \uparrow}^\dagger B_{\mathbf{k}, \uparrow} \rangle \right. \\
&\quad + (f_{\mathbf{k}} \beta_{\mathbf{k}} u_{\mathbf{k}}^- + g_{\mathbf{k}} \alpha_{\mathbf{k}} v_{\mathbf{k}}^-) (f_{\mathbf{k}}^* \alpha_{\mathbf{k}} u_{\mathbf{k}}^- + g_{\mathbf{k}}^* \beta_{\mathbf{k}} v_{\mathbf{k}}^-) \langle B_{\mathbf{k}+\mathbf{Q}, \uparrow}^\dagger B_{\mathbf{k}+\mathbf{Q}, \uparrow} \rangle \\
&\quad + (-f_{\mathbf{k}} \alpha_{\mathbf{k}} v_{\mathbf{k}}^+ - g_{\mathbf{k}} \beta_{\mathbf{k}} u_{\mathbf{k}}^+) (f_{\mathbf{k}}^* \beta_{\mathbf{k}} v_{\mathbf{k}}^+ + g_{\mathbf{k}}^* \alpha_{\mathbf{k}} u_{\mathbf{k}}^+) \langle B_{-\mathbf{k}, \uparrow}^\dagger B_{-\mathbf{k}, \uparrow} \rangle \\
&\quad + (f_{\mathbf{k}} \beta_{\mathbf{k}} v_{\mathbf{k}}^- - g_{\mathbf{k}} \alpha_{\mathbf{k}} u_{\mathbf{k}}^-) (f_{\mathbf{k}}^* \alpha_{\mathbf{k}} v_{\mathbf{k}}^- - g_{\mathbf{k}}^* \beta_{\mathbf{k}} u_{\mathbf{k}}^-) \langle B_{-\mathbf{k}+\mathbf{Q}, \uparrow}^\dagger B_{-\mathbf{k}+\mathbf{Q}, \uparrow} \rangle \\
&\quad - (f_{\mathbf{k}} \alpha_{\mathbf{k}} v_{\mathbf{k}}^+ + g_{\mathbf{k}} \beta_{\mathbf{k}} u_{\mathbf{k}}^+) (f_{\mathbf{k}}^* \beta_{\mathbf{k}} v_{\mathbf{k}}^+ + g_{\mathbf{k}}^* \alpha_{\mathbf{k}} u_{\mathbf{k}}^+) \langle B_{\mathbf{k}, \uparrow}^\dagger B_{\mathbf{k}, \uparrow} \rangle \\
&\quad - (f_{\mathbf{k}} \beta_{\mathbf{k}} v_{\mathbf{k}}^- - g_{\mathbf{k}} \alpha_{\mathbf{k}} u_{\mathbf{k}}^-) (-f_{\mathbf{k}}^* \alpha_{\mathbf{k}} v_{\mathbf{k}}^- + g_{\mathbf{k}}^* \beta_{\mathbf{k}} u_{\mathbf{k}}^-) \langle B_{\mathbf{k}+\mathbf{Q}, \uparrow}^\dagger B_{\mathbf{k}+\mathbf{Q}, \uparrow} \rangle \\
&\quad - (f_{\mathbf{k}} \alpha_{\mathbf{k}} u_{\mathbf{k}}^+ - g_{\mathbf{k}} \beta_{\mathbf{k}} v_{\mathbf{k}}^+) (f_{\mathbf{k}}^* \beta_{\mathbf{k}} u_{\mathbf{k}}^+ - g_{\mathbf{k}}^* \alpha_{\mathbf{k}} v_{\mathbf{k}}^+) \langle B_{-\mathbf{k}, \uparrow}^\dagger B_{-\mathbf{k}, \uparrow} \rangle \\
&\quad \left. - (-f_{\mathbf{k}} \beta_{\mathbf{k}} u_{\mathbf{k}}^- - g_{\mathbf{k}} \alpha_{\mathbf{k}} v_{\mathbf{k}}^-) (f_{\mathbf{k}}^* \alpha_{\mathbf{k}} u_{\mathbf{k}}^- + g_{\mathbf{k}}^* \beta_{\mathbf{k}} v_{\mathbf{k}}^-) \langle B_{-\mathbf{k}+\mathbf{Q}, \uparrow}^\dagger B_{-\mathbf{k}+\mathbf{Q}, \uparrow} \rangle \right], \\
&= \sum_{\mathbf{k}} \alpha_{\mathbf{k}} \beta_{\mathbf{k}} (|f_{\mathbf{k}}|^2 - |g_{\mathbf{k}}|^2) \left[((v_{\mathbf{k}}^-)^2 - (v_{\mathbf{k}}^+)^2) + ((v_{\mathbf{k}}^+)^2 - (u_{\mathbf{k}}^+)^2) n(E_{\mathbf{k}}^+) - ((v_{\mathbf{k}}^-)^2 - (u_{\mathbf{k}}^-)^2) n(E_{\mathbf{k}}^-) \right]. \quad (\text{B6})
\end{aligned}$$

Appendix C: Penetration Depth

The quantum mechanical electric current can be written as

$$\mathbf{J} = -\frac{e}{2m} (\psi^\dagger \mathbf{p} \psi - (\mathbf{p} \psi)^\dagger \psi) \quad (\text{C1})$$

Now in a magnetic field the momentum operator becomes $\mathbf{p} + e/c\mathbf{A}$, so that the current is

$$\begin{aligned}
\mathbf{J} &= -\frac{e}{2m} (\psi^\dagger (\mathbf{p} + e/c\mathbf{A}) \psi - [(\mathbf{p} + e/c(\mathbf{A}))\psi]^\dagger \psi) \\
&= -\frac{e}{2m} (\psi^\dagger \mathbf{p} \psi - (\mathbf{p} \psi)^\dagger \psi) - \frac{e^2 \mathbf{A}}{mc} \psi^\dagger \psi \quad (\text{C2})
\end{aligned}$$

The first term represents the current due to the normal electrons (paramagnetic current) and the second term is identified as the diamagnetic current which is contributed by the superconducting electrons n_s . The paramagnetic current (\mathbf{J}_n) has the tendency to cancel the diamagnetic current (\mathbf{J}_s). Therefore the velocity of the superconducting electrons are identified as $\mathbf{v}_s^* = \frac{e\mathbf{A}}{m^*c}$ where m^* , the band mass, is a 2×2 tensor in two dimensional space defined below.

The Fourier transformation of these quantities gives

$$\begin{aligned}
\mathbf{J}(\mathbf{q}) &= \int \mathbf{J}(\mathbf{r}) e^{-i\mathbf{q}\cdot\mathbf{r}} d^3\mathbf{r}, \\
\mathbf{a}(\mathbf{q}) &= \int \mathbf{A}(\mathbf{r}) e^{-i\mathbf{q}\cdot\mathbf{r}} d^3\mathbf{r}, \\
\mathbf{K}(\mathbf{q}) &= \int \mathbf{K}(\mathbf{r}) e^{-i\mathbf{q}\cdot\mathbf{r}} d^3\mathbf{r}, \quad (\text{C3})
\end{aligned}$$

which gives

$$\mathbf{J}(\mathbf{q}) = \mathbf{J}_n(\mathbf{q}) + \mathbf{J}_s(\mathbf{q}) = \mathbf{A}(\mathbf{q}) \cdot \vec{K}(\mathbf{q}), \quad (\text{C4})$$

where $\mathbf{K}(\mathbf{q})$ is called the response function. Now in an anisotropic system the response function becomes a 2×2 tensor as defined below

$$\begin{aligned}
\begin{pmatrix} J_x(\mathbf{q}) \\ J_y(\mathbf{q}) \end{pmatrix} &= \begin{pmatrix} J_{nx}(\mathbf{q}) + J_{sx}(\mathbf{q}) \\ J_{ny}(\mathbf{q}) + J_{sy}(\mathbf{q}) \end{pmatrix} \\
&= -\frac{c}{4\pi} \begin{pmatrix} K_{xx}(\mathbf{q}) & K_{xy}(\mathbf{q}) \\ K_{yx}(\mathbf{q}) & K_{yy}(\mathbf{q}) \end{pmatrix} \begin{pmatrix} a_x(\mathbf{q}) \\ a_y(\mathbf{q}) \end{pmatrix} \quad (\text{C5})
\end{aligned}$$

where at $\mathbf{q} = 0$, the penetration depth is related to K 's as

$$\lambda_{ij}^{-2}(T) = K_{ij}(0) \quad (\text{C6})$$

1. Paramagnetic Current, $\mathbf{J}_p(\mathbf{q})$

The first term \mathbf{J}_p arises due to normal electrons, which is often called the ‘‘paramagnetic current’’ term because it tends to cancel the diamagnetic current \mathbf{J}_d , which arises because of superconducting electrons. In the presence of an electromagnetic field (the field includes the effects of screening supercurrents), the canonical momentum is modified and the kinetic energy is $(\mathbf{p}^* - e\mathbf{A}/c)^2/2m^*$, where \mathbf{p}^* is the crystal momentum or the band momentum. Thus the resulting perturbation

Hamiltonian term is

$$\begin{aligned} H_I &= -\frac{e}{2c} \sum_i \frac{1}{m^*} (\mathbf{p}^* \cdot \mathbf{A} + \mathbf{A} \cdot \mathbf{p}^*) \\ &= -\frac{e}{c} \sum_i \mathbf{v}^* \cdot \mathbf{A} \end{aligned} \quad (C7)$$

The band momentum is defined as $\mathbf{p}^* = m^* \mathbf{v}^*$, where \mathbf{v}^* is the band velocity for the band $\xi_{\mathbf{k}}^{\pm}$. Note that the symbol $v_{\mathbf{k}}$ without a superscript of \pm is the band velocity, while with the superscript it gives the AFM coherence factors.

$$\begin{aligned} \mathbf{J}_p(0) &= -e\mathbf{v}^* n \\ &= -\frac{e}{\Omega} \sum_{\mathbf{k}} \left[\mathbf{v}_{\mathbf{k}} \langle c_{\mathbf{k},\uparrow}^\dagger c_{\mathbf{k},\uparrow} \rangle + \mathbf{v}_{\mathbf{k}+\mathbf{Q}} \langle c_{\mathbf{k}+\mathbf{Q},\uparrow}^\dagger c_{\mathbf{k}+\mathbf{Q},\uparrow} \rangle - \mathbf{v}_{\mathbf{k}} \langle c_{-\mathbf{k},\downarrow}^\dagger c_{-\mathbf{k},\downarrow} \rangle - \mathbf{v}_{\mathbf{k}+\mathbf{Q}} \langle c_{-\mathbf{k}-\mathbf{Q},\downarrow}^\dagger c_{-\mathbf{k}-\mathbf{Q},\downarrow} \rangle \right] \\ &= -\frac{e}{c\Omega} \mathbf{a}(0) \sum_{\mathbf{k}} \left[f_{\mathbf{k}}^2 (\mathbf{v}_{\mathbf{k}} \alpha_{\mathbf{k}}^2 + \mathbf{v}_{\mathbf{k}+\mathbf{Q}} \beta_{\mathbf{k}}^2) + g_{\mathbf{k}}^2 (\mathbf{v}_{\mathbf{k}} \beta_{\mathbf{k}}^2 + \mathbf{v}_{\mathbf{k}+\mathbf{Q}} \alpha_{\mathbf{k}}^2) \right] \left(\langle B_{\mathbf{k},\uparrow}^\dagger B_{\mathbf{k},\uparrow} \rangle - \langle B_{-\mathbf{k},\downarrow}^\dagger B_{-\mathbf{k},\downarrow} \rangle \right) \\ &\quad + \left[f_{\mathbf{k}}^2 (\mathbf{v}_{\mathbf{k}} \beta_{\mathbf{k}}^2 + \mathbf{v}_{\mathbf{k}+\mathbf{Q}} \alpha_{\mathbf{k}}^2) + g_{\mathbf{k}}^2 (\mathbf{v}_{\mathbf{k}} \alpha_{\mathbf{k}}^2 + \mathbf{v}_{\mathbf{k}+\mathbf{Q}} \beta_{\mathbf{k}}^2) \right] \left(\langle B_{\mathbf{k}+\mathbf{Q},\uparrow}^\dagger B_{\mathbf{k}+\mathbf{Q},\uparrow} \rangle - \langle B_{-\mathbf{k}-\mathbf{Q},\downarrow}^\dagger B_{-\mathbf{k}-\mathbf{Q},\downarrow} \rangle \right) \\ &= -\frac{e}{c\Omega} \mathbf{a}(0) \sum_{\mathbf{k}} \mathbf{V}_{\mathbf{k}}^+ \left(\langle B_{\mathbf{k},\uparrow}^\dagger B_{\mathbf{k},\uparrow} \rangle - \langle B_{-\mathbf{k},\downarrow}^\dagger B_{-\mathbf{k},\downarrow} \rangle \right) + \mathbf{V}_{\mathbf{k}}^- \left(\langle B_{\mathbf{k}+\mathbf{Q},\uparrow}^\dagger B_{\mathbf{k}+\mathbf{Q},\uparrow} \rangle - \langle B_{-\mathbf{k}-\mathbf{Q},\downarrow}^\dagger B_{-\mathbf{k}-\mathbf{Q},\downarrow} \rangle \right). \end{aligned} \quad (C8)$$

Here Ω is the unit cell volume. $\mathbf{V}_{\mathbf{k}}^+ = C_{\mathbf{k}} \mathbf{v}_{\mathbf{k}} + C_{\mathbf{k}+\mathbf{Q}} \mathbf{v}_{\mathbf{k}+\mathbf{Q}}$ and $\mathbf{V}_{\mathbf{k}}^- = \mathbf{V}_{\mathbf{k}+\mathbf{Q}}^+$, and $C_{\mathbf{k}} = |f_{\mathbf{k}}|^2 \alpha_{\mathbf{k}}^2 + |g_{\mathbf{k}}|^2 \beta_{\mathbf{k}}^2$. Now the probability of excitation of the fermion quasiparticles in an electromagnetic field in the thermal equilibrium is the usual Fermi function in the corresponding energy level sifted by the electromagnetic field. In the limit of small $\mathbf{a}(0)$, we can expand the Fermi function in Taylor's series and keeping only the first term we get,

$$\begin{aligned} n(E_{\mathbf{k}\pm}^\nu) &= n(E_{\mathbf{k}}^\nu \mp \frac{e}{c} \mathbf{v}_{\mathbf{k}}^\nu \cdot \mathbf{a}(0)) \\ &\approx n(E_{\mathbf{k}}^\nu) \mp \frac{e}{c} \left(\frac{\partial n(E_{\mathbf{k}}^\nu)}{\partial E_{\mathbf{k}}^\nu} \right) \mathbf{V}_{\mathbf{k}}^\nu \cdot \mathbf{a}(0). \end{aligned} \quad (C9)$$

Here $\nu = \pm$ are two quasiparticle bands. Then adding and subtracting the fermi functions we have

$$n(E_{\mathbf{k}+}^\nu) + n(E_{\mathbf{k}-}^\nu) \approx 2n(E_{\mathbf{k}}^\nu) \quad (C10)$$

$$n(E_{\mathbf{k}+}^\nu) - n(E_{\mathbf{k}-}^\nu) \approx -\frac{2e}{c} \left(\frac{\partial n(E_{\mathbf{k}}^\nu)}{\partial E_{\mathbf{k}}^\nu} \right) \mathbf{V}_{\mathbf{k}}^\nu \cdot \mathbf{a}(0) \quad (C11)$$

Substituting Eq. C11 in Eq. C8, we get the paramagnetic current as

$$\begin{aligned} \mathbf{J}_p(0) &= -\frac{2e^2}{c\Omega} \sum_{\mathbf{k},\nu} \mathbf{V}^\nu \left(\mathbf{V}^\nu \cdot \mathbf{a}(0) \right) \left(-\frac{\partial f(E_{\mathbf{k}}^\nu)}{\partial E_{\mathbf{k}}^\nu} \right) \\ &= -\frac{e^2}{c\Omega} \frac{\beta}{2} \sum_{\mathbf{k},\nu} \mathbf{V}^\nu \left(\mathbf{V}^\nu \cdot \mathbf{a}(0) \right) \text{sech}^2(\beta E_{\mathbf{k}}^\nu / 2) \end{aligned} \quad (C12)$$

2. Diamagnetic Current

Let us define

$$\begin{aligned} \frac{1}{M_{\mathbf{k}i,j}^+} &= C_{\mathbf{k}} \left(\frac{1}{m_{\mathbf{k}i,j}} \right) + C_{\mathbf{k}+\mathbf{Q}} \left(\frac{1}{m_{\mathbf{k}+\mathbf{Q}i,j}} \right), \\ \frac{1}{m_{\mathbf{k}i,j}^\nu} &= 4f_{\mathbf{k}} g_{\mathbf{k}} \alpha_{\mathbf{k}} \beta_{\mathbf{k}} u_{\mathbf{k}}^\nu v_{\mathbf{k}}^\nu \left(\frac{1}{m_{\mathbf{k}i,j}^*} + \frac{1}{m_{\mathbf{k}+\mathbf{Q}i,j}^*} \right), \end{aligned} \quad (C13)$$

and $\frac{1}{M_{\mathbf{k}i,j}^-} = \frac{1}{M_{\mathbf{k}+\mathbf{Q}i,j}^+}$. Then the i^{th} component of the diamagnetic Current is

$$\begin{aligned}
J_{di}(0) &= -\frac{e^2}{c} \sum_{j=1}^2 \left(\frac{1}{m_{i,j}^*} \right) a_j(0) n \\
&= -\frac{e^2}{c\Omega} \sum_{j=1}^2 a_j(0) \sum_{\mathbf{k}}' \left[\left(\frac{1}{m_{\mathbf{k}i,j}^*} \right) \langle c_{\mathbf{k},\uparrow}^\dagger c_{\mathbf{k},\uparrow} \rangle + \left(\frac{1}{m_{\mathbf{k}+\mathbf{Q}i,j}^*} \right) \langle c_{\mathbf{k}+\mathbf{Q},\uparrow}^\dagger c_{\mathbf{k}+\mathbf{Q},\uparrow} \rangle \right. \\
&\quad \left. + \left(\frac{1}{m_{\mathbf{k}i,j}^*} \right) \langle c_{-\mathbf{k},\downarrow}^\dagger c_{-\mathbf{k},\downarrow} \rangle + \left(\frac{1}{m_{\mathbf{k}+\mathbf{Q}i,j}^*} \right) \langle c_{-\mathbf{k}-\mathbf{Q},\downarrow}^\dagger c_{-\mathbf{k}-\mathbf{Q},\downarrow} \rangle \right] \\
&= -\frac{e^2}{c\Omega} \sum_{j=1}^2 a_j(0) \sum_{\mathbf{k}}' \left[\left(\frac{1}{m_{i,j}^*} \right) \left\{ (f_{\mathbf{k}} \alpha_{\mathbf{k}} u_{\mathbf{k}}^+ - g_{\mathbf{k}} \beta_{\mathbf{k}} v_{\mathbf{k}}^+)^2 - (f_{\mathbf{k}} \alpha_{\mathbf{k}} v_{\mathbf{k}}^+ + g_{\mathbf{k}} \beta_{\mathbf{k}} u_{\mathbf{k}}^+)^2 \right\} \right. \\
&\quad \left. + \left(\frac{1}{m_{\mathbf{k}+\mathbf{Q}i,j}^*} \right) \left\{ (f_{\mathbf{k}} \beta_{\mathbf{k}} u_{\mathbf{k}}^+ - g_{\mathbf{k}} \alpha_{\mathbf{k}} v_{\mathbf{k}}^+)^2 - (f_{\mathbf{k}} \beta_{\mathbf{k}} v_{\mathbf{k}}^+ + g_{\mathbf{k}} \alpha_{\mathbf{k}} u_{\mathbf{k}}^+)^2 \right\} \right] \left(\langle B_{\mathbf{k},\uparrow}^\dagger B_{\mathbf{k},\uparrow} \rangle + \langle B_{-\mathbf{k},\downarrow}^\dagger B_{-\mathbf{k},\downarrow} \rangle \right) \\
&\quad + 2 \left(\frac{1}{m_{i,j}^*} \right) (f_{\mathbf{k}} \alpha_{\mathbf{k}} v_{\mathbf{k}}^+ + g_{\mathbf{k}} \beta_{\mathbf{k}} u_{\mathbf{k}}^+)^2 + 2 \left(\frac{1}{m_{\mathbf{k}+\mathbf{Q}i,j}^*} \right) \mathbf{v}_{\mathbf{k}+\mathbf{Q}} (f_{\mathbf{k}} \beta_{\mathbf{k}} v_{\mathbf{k}}^+ + g_{\mathbf{k}} \alpha_{\mathbf{k}} u_{\mathbf{k}}^+)^2 \\
&\quad + \left[\left(\frac{1}{m_{i,j}^*} \right) \left\{ (f_{\mathbf{k}} \beta_{\mathbf{k}} u_{\mathbf{k}}^- + g_{\mathbf{k}} \alpha_{\mathbf{k}} v_{\mathbf{k}}^-)^2 - \left(\frac{1}{m_{i,j}^*} \right) (f_{\mathbf{k}} \beta_{\mathbf{k}} v_{\mathbf{k}}^- - g_{\mathbf{k}} \alpha_{\mathbf{k}} u_{\mathbf{k}}^-)^2 \right\} \right. \\
&\quad \left. + \left(\frac{1}{m_{\mathbf{k}+\mathbf{Q}i,j}^*} \right) \left\{ (f_{\mathbf{k}} \alpha_{\mathbf{k}} u_{\mathbf{k}}^- + g_{\mathbf{k}} \beta_{\mathbf{k}} v_{\mathbf{k}}^-)^2 - (f_{\mathbf{k}} \alpha_{\mathbf{k}} v_{\mathbf{k}}^- - g_{\mathbf{k}} \beta_{\mathbf{k}} u_{\mathbf{k}}^-)^2 \right\} \right] \left(\langle B_{\mathbf{k}+\mathbf{Q},\uparrow}^\dagger B_{\mathbf{k}+\mathbf{Q},\uparrow} \rangle + \langle B_{-\mathbf{k}-\mathbf{Q},\downarrow}^\dagger B_{-\mathbf{k}-\mathbf{Q},\downarrow} \rangle \right) \\
&\quad + 2 \left(\frac{1}{m_{i,j}^*} \right) (f_{\mathbf{k}} \beta_{\mathbf{k}} v_{\mathbf{k}}^- - g_{\mathbf{k}} \alpha_{\mathbf{k}} u_{\mathbf{k}}^-)^2 + 2 \left(\frac{1}{m_{\mathbf{k}+\mathbf{Q}i,j}^*} \right) (f_{\mathbf{k}} \alpha_{\mathbf{k}} v_{\mathbf{k}}^- - g_{\mathbf{k}} \beta_{\mathbf{k}} u_{\mathbf{k}}^-)^2 \\
&= -\frac{e^2}{c\Omega} \sum_{j=1}^2 a_j(0) \sum_{\mathbf{k}}' \\
&\quad f_{\mathbf{k}}^2 \left(\left(\frac{1}{m_{i,j}^*} \right) \alpha_{\mathbf{k}}^2 + \left(\frac{1}{m_{\mathbf{k}+\mathbf{Q}i,j}^*} \right) \beta_{\mathbf{k}}^2 \right) \left[2(v_{\mathbf{k}}^+)^2 + ((u_{\mathbf{k}}^+)^2 - (v_{\mathbf{k}}^+)^2) (1 - \langle B_{\mathbf{k},\uparrow}^\dagger B_{\mathbf{k},\uparrow} \rangle - \langle B_{-\mathbf{k},\downarrow}^\dagger B_{-\mathbf{k},\downarrow} \rangle) \right] \\
&\quad + g_{\mathbf{k}}^2 \left(\left(\frac{1}{m_{i,j}^*} \right) \beta_{\mathbf{k}}^2 + \left(\frac{1}{m_{\mathbf{k}+\mathbf{Q}i,j}^*} \right) \alpha_{\mathbf{k}}^2 \right) \left[2(u_{\mathbf{k}}^+)^2 - ((u_{\mathbf{k}}^+)^2 - (v_{\mathbf{k}}^+)^2) (1 - \langle B_{\mathbf{k},\uparrow}^\dagger B_{\mathbf{k},\uparrow} \rangle - \langle B_{-\mathbf{k},\downarrow}^\dagger B_{-\mathbf{k},\downarrow} \rangle) \right] \\
&\quad + 4f_{\mathbf{k}}g_{\mathbf{k}}\alpha_{\mathbf{k}}\beta_{\mathbf{k}}u_{\mathbf{k}}^+v_{\mathbf{k}}^+ \left(\frac{1}{m_{\mathbf{k}i,j}^*} + \frac{1}{m_{\mathbf{k}+\mathbf{Q}i,j}^*} \right) (1 - \langle B_{\mathbf{k},\uparrow}^\dagger B_{\mathbf{k},\uparrow} \rangle - \langle B_{-\mathbf{k},\downarrow}^\dagger B_{-\mathbf{k},\downarrow} \rangle) \\
&\quad + f_{\mathbf{k}}^2 \left(\left(\frac{1}{m_{i,j}^*} \right) \beta_{\mathbf{k}}^2 + \left(\frac{1}{m_{\mathbf{k}+\mathbf{Q}i,j}^*} \right) \alpha_{\mathbf{k}}^2 \right) \left[2(v_{\mathbf{k}}^+)^2 + ((u_{\mathbf{k}}^+)^2 - (v_{\mathbf{k}}^+)^2) \right. \\
&\quad \left. \times (1 - \langle B_{\mathbf{k}+\mathbf{Q},\uparrow}^\dagger B_{\mathbf{k}+\mathbf{Q},\uparrow} \rangle - \langle B_{-\mathbf{k}-\mathbf{Q},\downarrow}^\dagger B_{-\mathbf{k}-\mathbf{Q},\downarrow} \rangle) \right] \\
&\quad + g_{\mathbf{k}}^2 \left(\left(\frac{1}{m_{i,j}^*} \right) \alpha_{\mathbf{k}}^2 + \left(\frac{1}{m_{\mathbf{k}+\mathbf{Q}i,j}^*} \right) \beta_{\mathbf{k}}^2 \right) \left[2(u_{\mathbf{k}}^+)^2 - ((u_{\mathbf{k}}^+)^2 - (v_{\mathbf{k}}^+)^2) \right. \\
&\quad \left. \times (1 - \langle B_{\mathbf{k}+\mathbf{Q},\uparrow}^\dagger B_{\mathbf{k}+\mathbf{Q},\uparrow} \rangle - \langle B_{-\mathbf{k}-\mathbf{Q},\downarrow}^\dagger B_{-\mathbf{k}-\mathbf{Q},\downarrow} \rangle) \right] \\
&\quad + 4f_{\mathbf{k}}g_{\mathbf{k}}\alpha_{\mathbf{k}}\beta_{\mathbf{k}}u_{\mathbf{k}}^-v_{\mathbf{k}}^- \left(\frac{1}{m_{\mathbf{k}i,j}^*} + \frac{1}{m_{\mathbf{k}+\mathbf{Q}i,j}^*} \right) (1 - \langle B_{\mathbf{k}+\mathbf{Q},\uparrow}^\dagger B_{\mathbf{k}+\mathbf{Q},\uparrow} \rangle - \langle B_{-\mathbf{k}-\mathbf{Q},\downarrow}^\dagger B_{-\mathbf{k}-\mathbf{Q},\downarrow} \rangle) \\
&= -\frac{e^2}{c\Omega} \sum_{j=1}^2 a_j(0) \sum_{\mathbf{k}}' \sum_{\nu=\pm} \left(\frac{1}{M_{\mathbf{k}i,j}^\nu} \right) \left(1 - \frac{E_{\mathbf{k}}^\pi + E_{\mathbf{k}}^m}{E_{\mathbf{k}}^\nu} \tanh(\beta E_{\mathbf{k}}^\nu/2) \right) + \left(\frac{1}{m_{\mathbf{k}i,j}^\nu} \right) \tanh(\beta E_{\mathbf{k}}^\nu/2). \tag{C14}
\end{aligned}$$

Therefore using Eq. C12 and C14, we get from Eq. C4 that the penetration depth in C.G.S unit system at any temperature

T as given in Eq. 6.

- [1] A. Ino, C. Kim, M. Nakamura, T. Yoshida, T. Mizokawa, Z.-X. Shen, A. Fujimori, T. Kakeshita, H. Eisaki, and S. Uchida, Electronic structure of $\text{La}_{2-x}\text{Sr}_x\text{CuO}_4$ in the vicinity of the superconductor-insulator transition. *Phys. Rev. B* **62**, 4137 (2000).
- [2] K. M. Shen, *et al.*, Fully gapped single-particle excitations in lightly doped cuprates. *Phys. Rev. B* **69**, 054503 (2004).
- [3] K. Tanaka, W. S. Lee, D. H. Lu, A. Fujimori, T. Fujii, Risdiana, I. Terasaki, D. J. Scalapino, T. P. Devereaux, Z. Hussain, and Z.-X. Shen, Distinct Fermi-momentum-dependent energy gaps in deeply underdoped Bi2212 . *Science* **314**, 1910 (2006).
- [4] I. M. Vishik, *et al.* Phase competition in trisected superconducting dome. *Proc. Nat. Acad. Sci. (USA)* **109**, 18332 (2012).
- [5] E. Razzoli, G. Drachuck, A. Keren, M. Radovic, N. C. Plumb, J. Chang, Y.-B. Huang, H. Ding, J. Mesot, and M. Shi, Evolution from a nodeless gap to $d_{x^2-y^2}$ -wave in underdoped $\text{La}_{2-x}\text{Sr}_x\text{CuO}_4$. *Phys. Rev. Lett.* **110**, 047004 (2013).
- [6] Y. Peng, J. Meng, D. Mou, J. He, L. Zhao, Y. Wu, G. Liu, X. Dong, S. He, J. Zhang, X. Wang, Q. Peng, Z. Wang, S. Zhang, F. Yang, C. Chen, Z. Xu, T. K. Lee, X. J. Zhou, Disappearance of nodal gap across the insulator/superconductor transition in a copper-oxide superconductor. *Nat. Commun.* **4**, 2459 (2013).
- [7] D. Gustafsson, D. Golubev, M. Fogelström, T. Claeson, S. Kubatkin, T. Bauch, and F. Lombardi, Fully gapped superconductivity in a nanometre-size $\text{YBa}_2\text{Cu}_3\text{O}_{7\delta}$ island enhanced by a magnetic field. *Nat. Nanotechnology* **8**, 25-30 (2013).
- [8] T. Das, R. S. Markiewicz, and A. Bansil, Nodeless d -wave Superconducting pairing due to residual antiferromagnetism in underdoped $\text{Pr}_{2-x}\text{Ce}_x\text{CuO}_{4\delta}$. *Phys. Rev. Lett* **98**, 197004 (2007).
- [9] T. Das, and A. V. Balatsky, Stripes, spin resonance, and nodeless d -wave pairing symmetry in Fe_2Se_2 -based layered superconductors. *Phys. Rev. B* **84**, 014521 (2011).
- [10] W. Chen, G. Khaliullin, and O. P. Sushkov, Coulomb disorder effects on angle-resolved photoemission and nuclear quadrupole resonance spectra in cuprates. *Phys. Rev. B* **80**, 094519 (2009).
- [11] A. M. Black-Schaffer, D. S. Golubev, T. Bauch, F. Lombardi, and M. Fogelström, *Phys. Rev. Lett.* **110**, 197001 (2013).
- [12] Y.-M. Lu, T. Xiang, and D.-H. Lee, Can deeply underdoped superconducting cuprates be topological superconductors? arXiv:1311.5892.
- [13] S. Sakai, and M. Civelli, Doping evolution of the electron-hole asymmetric s -wave pseudogap in underdoped high-Tc cuprate superconductors. arXiv:1311.6945.
- [14] A. Go, and A. J. Millis, Spatial correlations and the insulating phase of the high-Tc cuprates: insights from a configuration interaction based solver for dynamical mean field theory. arXiv:1311.6819.
- [15] S. Shimizu, S.-i. Tabata, S. Iwai, H. Mukuda, and Y. Kitaoka, High-temperature superconductivity and antiferromagnetism in multilayer cuprates: Cu and F NMR on five-layer $\text{BaCaCuO}(\text{F},\text{O})$. *Phys. Rev. B* **85**, 024528 (2012).
- [16] S. Shimizu, S.-i. Tabata, H. Mukuda, Y. Kitaoka, P. M. Shirage, H. i Kito, and A. Iyo, Antiferromagnetism, superconductivity, and pseudogap in three-layered high-Tc cuprates $\text{Ba}_2\text{Ca}_2\text{Cu}_3\text{O}_6(\text{F},\text{O})_2$ probed by Cu-NMR, *Phys. Rev. B* **83**, 214514 (2011).
- [17] H. Mukuda, S. Shimizu, A. Iyo, and Y. Kitaoka, High-Tc superconductivity and antiferromagnetism in multilayered copper oxides A new paradigm of superconducting mechanism. *J. Phys. Soc. Jpn.* **81**, 011008 (2012).
- [18] S.-H. Baek, T. Loew, V. Hinkov, C. T. Lin, B. Keimer, B. Büchner, and H.-J. Grafe, Evidence of a critical hole concentration in underdoped YBaCuO single crystals revealed by Cu NMR, *Phys. Rev B* **86**, 220504(R) (2012).
- [19] D. Haug, V. Hinkov, Y. Sidis, P. Bourges, N. B. Christensen, A. Ivanov, T. Keller, C. T. Lin and B. Keimer, *New J. Phys.* **12**, 105006 (2010).
- [20] V. Balédent, D. Haug, Y. Sidis, V. Hinkov, C. T. Lin, and P. Bourges, *Phys. Rev. B* **83**, 104504 (2011)
- [21] G.C. Psaltakis and E.W. Fenton, *J. Phys. C* **16**, 3913 (1983); B. Kyung, *Phys. Rev. B* **62**, 9083 (2000).
- [22] S.-C. Zhang, A unified theory based on $\text{SO}(5)$ symmetry of superconductivity and antiferromagnetism. *Science* **275** 1089-1096 (1997).
- [23] P. Fulde, and R. A. Ferrell, Superconductivity in a strong spin-exchange field. *Phys. Rev.* **135**, A550 (1964); A. I. Larkin, and Yu N. Ovchinnikov, *Zh. Eksp. Teor. Fiz.* **47**, 1136 (1964); A. I. Larkin, and Yu N. Ovchinnikov, Inhomogeneous state of superconductors. *Sov. Phys. JETP* **20**, 762 (1965).
- [24] While a single band model is valid for the low-energy physics of most of the cuprates, other bands such as materials specific CuO chain state[25] or HgO like bands[26] are required to be included in YBCO and HgCCO cuprates, respectively.
- [25] T. Das, Electron-like Fermi surface and in-plane anisotropy due to chain states in $\text{YBa}_2\text{Cu}_3\text{O}_{7\delta}$ superconductors. *Phys. Rev. B* **86**, 064527 (2012).
- [26] T. Das, $Q=0$ collective modes originating from the low-lying Hg-O band in superconducting $\text{HgBa}_2\text{CuO}_{4+\delta}$. *Phys. Rev. B* **86**, 054518 (2012).
- [27] R. S. Markiewicz, S. Sahrakorpi, M. Lindroos, Hsin Lin, and A. Bansil, One-band tight-binding model parametrization of the high-Tc cuprates including the effect of k_z dispersion. *Phys. Rev. B* **72**, 054519 (2005).
- [28] T. Das, R.S. Markiewicz, and A. Bansil, Competing order scenario of two-gap behavior in hole-doped cuprates. *Phys. Rev. B* **77**, 134516 (2008).
- [29] L. Fu, and E. Berg, Odd-parity topological superconductors: Theory and application to $\text{Cu}_x\text{Bi}_2\text{Se}_3$. *Phys. Rev. Lett.* **105**, 097001 (2010).
- [30] A. Aperis, G. Varelogiannis, and P. B. Littlewood, Magnetic-field-induced pattern of coexisting condensates in the superconducting state of CeCoIn_5 . *Phys. Rev. Lett.* **104**, 216403 (2010).
- [31] R. S. Markiewicz and M. T. Vaughn, Classification of the Van Hove scenario as an $\text{SO}(8)$ spectrum-generating algebra. *Phys. Rev. B* **57**, R14052 (1998).
- [32] B. Kyung, Mean-field study of the interplay between antiferromagnetism and d -wave superconductivity. *Phys. Rev. B*, **62**, 9083 (2000).